Sapphire++ — MHD: A finite element MHD code for astrophysical plasmas with energetic particles

F. Schulze[1], N. Schween[1], B. Reville[1]

[1]*Max-Planck-Institut für Kernphysik, Heidelberg, Germany*

1. Introduction

The evolution of astrophysical plasmas is often driven by cosmic-ray (CR) currents. Close to their nominal sources such as supernova remnants (SNRs), and on galactic scales, CRs play a vital role in the driving turbulence and winds. Simulating these effects in large systems is a challenging multi-scale problem, as one needs to capture physical phenomena occurring on vastly different scales. In some scenarios, like the escape of CRs from sources (e.g. SNRs), characteristic quantities can vary by many orders of magnitude.

To address these open questions, we developed `Sapphire++` [6]. Its goal is to combine and couple simulations of the background plasma with energetic CRs. We use a pseudo-spectral method to solve the Vlasov-Fokker-Planck (VFP) equation for energetic particles [5]. Utilising a decomposition of the distribution function into spherical harmonics, the dimensionality of the problem is reduced. When combined with a discontinuous Galerkin (DG) method this allows for effective multi-scale simulations.

Here we present `Sapphire++`— MHD, the magnetohydrodynamics (MHD) module for the thermal plasma.

2. Sapphire++ — MHD

We solve the equations of ideal-MHD, with the possibility for CR source terms. In conservative form, this reads

$$\frac{\partial \mathbf{w}}{\partial t} + \nabla \cdot \mathbf{F}(\mathbf{w}) = \mathbf{S}_{\mathrm{CR}} \tag{1}$$

with the MHD state vector $\mathbf{w} = \left(\rho,\, \mathbf{p},\, \mathcal{E},\, \mathbf{B}\right)^T$, and associated flux $\mathbf{F}$. Here, ρ is the density, $\mathbf{p} = \rho\mathbf{u}$ the plasma momentum, $\mathcal{E}$ the energy density, and $\mathbf{B}$ the magnetic field. The source term $\mathbf{S}_{\mathrm{CR}}$ represents coupling with an external CR flux.

To solve this non-linear system of equations, we employ the discontinuous Galerkin finite element (DG-FE) method using the `deal.II` library [1]. We choose nodal Lagrange polynomials as basis functions, combined with a local Lax-Friedrichs flux. Time stepping is performed

using forward Euler (FE) or second/fourth order explicit Runge-Kutta (ERK2/ERK4) methods. The methods are subject to CFL condition for stability, which for DG reads,

$$\Delta t \leq \Delta t_{\mathrm{CFL}} = C \frac{\Delta x}{(2k+1)\lambda_{\max}},$$

with Δx the cell size, k the polynomial degree of the basis functions, $\lambda_{\max}$ the maximum eigenvalue and C the Courant number.

To ensure stability at shocks, we use a TVDM slope limiter [2]. This reduces the spatial order of the solution, we therefore combine it with the KXRCF shock indicator [4] to only limit at shocks, and not smooth parts of the solution. The divergence free condition for the magnetic field, $\nabla \cdot \mathbf{B} = 0$, is enforced using hyperbolic divergence cleaning (HDC). Similar methods have been explored in [3].

3. Results

To validate `Sapphire++`— MHD, we present a number of numerical test cases.

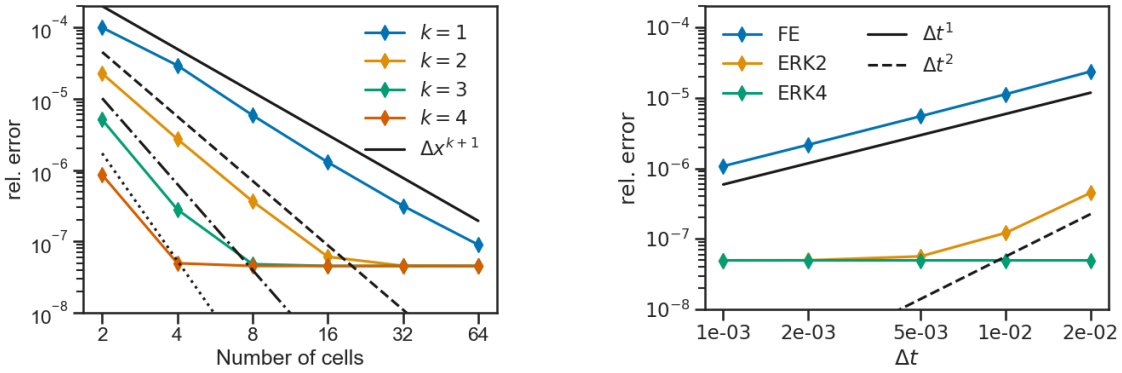

(a) Convergence with number of cells, using ERK4 with $C = 0.8$. It can be seen the convergence order is $k + 1$ for a polynomial basis of order k.

(b) Convergence order with time step size Δt, using $N = 4$ cells with polynomial degree $k = 4$. Numerical accuracy is reached at $\sim 5 \times 10^{-8}$.

Fig. 1: Convergence study for linear sound wave.

First, we study the convergence order using linear sound waves. We set up a 1 dimensional periodic box of length $L = 2$, with a left moving sound wave with sound speed $c_s = 1$ and compare the solution after one period $T = 2$. The results are presented in Fig. 1. We observe the expected convergence behaviour of order Δx^{k+1} with the polynomial degree of the basis functions k. Numerical accuracy is reached at $\sim 5 \times 10^{-8}$. Studying the temporal convergence, the expected behaviour of Δt and Δt^2 arises for FE and ERK2 respectively. The ERK4 method is limited by the numerical accuracy of $\sim 5 \times 10^{-8}$, so no convergence behaviour emerges.

Next, we assess effectiveness of the slope limiter and shock indicator using a spherical hy-

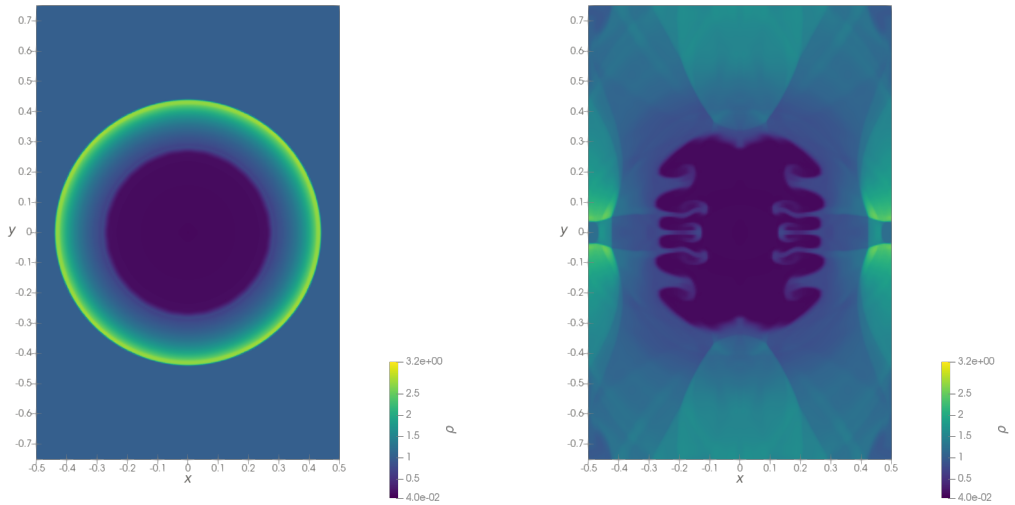

Fig. 2: Spherical blast wave at $t = 0.2$ (left) and $t = 1.5$ (right). We use 200×300 cells with periodic boundary conditions and $k = 1$.

drodynamical blast wave. The initial condition is a region of radius $r = 0.1$ with increased pressure $P = 10$ in an ambient medium $P = 0.1$. Fig. 2 shows the early time evolution at $t = 0.2$, and the chaotic late time ($t = 1.5$). For early times, an outwards travelling spherical shock wave emerges. The KXRCF indicator is able to identify this feature as a shock, so that the slope limiter is activated and damps the spurious Gibbs oscillations. We note that the spherical nature of the shock is well-preserved. At late times the shocks from both sides start to interact due to the periodic boundary conditions, leading to chaotic behaviour.

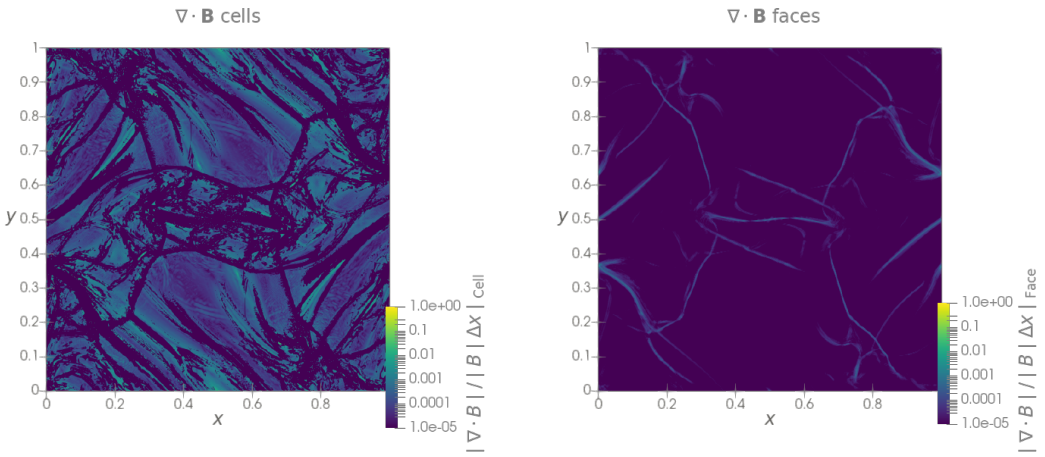

Fig. 3: Magnetic divergence for the Orszag-Tang vortex. We use 512×512 cells, and $k = 1$ in `Sapphire++`— MHD. The left side shows the contribution to magnetic divergence form the cell interiors, the right side the condition form cell faces.

Last, we verify that the chosen HDC method is sufficient to impose the divergence free condition, $\nabla \cdot \mathbf{B}$. A common test-case is the Orszag-Tang vortex, which starts with an initial field with

waves in the magnetic field components before transitioning to 2D MHD turbulence [3]. In DG methods, the divergence has two contributions, one from the cell integrals of the basis functions, and one from the jump of the normal component across cell faces. These two contributions are presented in Fig. 3, using a normalized measure of the magnetic divergence, $\frac{|\nabla \cdot B|}{|B|}\Delta x$, where $|\nabla \cdot B|$ is the cell/face integral of the absolute value of the magnetic divergence [3, App. C], While the total divergence stays below the per-mil level, the dominant contribution comes from the cell interiors. This hints that a different choice of basis functions, e.g. a locally divergence free basis, could improve accuracy.

4. Conclusions and Outlook

We presented `Sapphire++`— MHD, a new DG-MHD code. `Sapphire++`— MHD was validated using multiple test examples.

The next steps are to couple the MHD module with the VPF module in `Sapphire++`, to enable self-consistent simulations.

References

[1] Pasquale C. Africa et al. ‘‘The Deal.II Library, Version 9.6’’. In: *Journal of Numerical Mathematics* (Dec. 1, 2024). DOI: 10.1515/jnma-2024-0137.

[2] Bernardo Cockburn. ‘‘An Introduction to the Discontinuous Galerkin Method for Convection-Dominated Problems’’. In: Bernardo Cockburn et al. Springer Berlin Heidelberg, 1998. ISBN: 978-3-540-64977-9. DOI: 10.1007/BFb0096353.

[3] Thomas Guillet et al. ‘‘High-Order Magnetohydrodynamics for Astrophysics with an Adaptive Mesh Refinement Discontinuous Galerkin Scheme’’. In: *Monthly Notices of the Royal Astronomical Society* (May 1, 2019). DOI: 10.1093/mnras/stz314.

[4] L. Krivodonova et al. ‘‘Shock Detection and Limiting with Discontinuous Galerkin Methods for Hyperbolic Conservation Laws’’. In: *Applied Numerical Mathematics* (Mar. 1, 2004). DOI: 10.1016/j.apnum.2003.11.002.

[5] Nils W. Schween and Brian Reville. ‘‘Using Spherical Harmonics to Solve the Boltzmann Equation: An Operator-Based Approach’’. In: *Monthly Notices of the Royal Astronomical Society* (Apr. 11, 2024). DOI: 10.1093/mnras/stae596.

[6] Nils W. Schween, Florian Schulze, and Brian Reville. ‘‘Sapphire++: A Particle Transport Code Combining a Spherical Harmonic Expansion and the Discontinuous Galerkin Method’’. In: *Journal of Computational Physics* (Feb. 15, 2025). DOI: 10.1016/j.jcp.2024.113690.